Minerals **2015**, *5*, 61-79; doi:10.3390/min5010061

OPEN ACCESS

minerals

ISSN 2075-163X
www.mdpi.com/journal/minerals

Article

Advances in Trace Element "Fingerprinting" of Gem Corundum, Ruby and Sapphire, Mogok Area, Myanmar

F. Lin Sutherland [1,2,*], Khin Zaw [3], Sebastien Meffre [3], Tzen-Fui Yui [4] and Kyaw Thu [5]

[1] School of Science and Health, University of Western Sydney, North Parramatta Campus, Sydney, Penrith PO NSW 2075, Australia
[2] Geoscience, Australian Museum, 6 College Street, Sydney, NSW 2010, Australia
[3] CODES ARC Centre of Excellence in Ore Deposits, University of Tasmania, Hobart, Tas 7001, Australia; E-Mails: khin.zaw@utas.edu.au (K.Z.); sebastien.meffre@utas.edu.au (S.M.)
[4] Institute of Earth Sciences, Academia Sinica, Nankang 115, Taipei, Taiwan; E-Mail: tfyui@earth.sinica.edu.tw
[5] Geology Department, Yangon University, Yangon 11041, Myanmar; E-Mail: macle45@gmail.com

* Author to whom correspondence should be addressed; E-Mail: l.sutherland@uws.edu.au or lin.sutherland@austmus.gov.au; Tel.: +61-2-9685-9988; Fax: +61-2-9685-1195.

Academic Editor: Ian Graham

Received: 26 June 2014 / Accepted: 10 December 2014 / Published: 30 December 2014

Abstract: Mogok gem corundum samples from twelve localities were analyzed for trace element signatures (LA-ICP-MS method) and oxygen isotope values ($\delta^{18}O$, by laser fluorination). The study augmented earlier findings on Mogok gem suites that suggested the Mogok tract forms a high vanadium gem corundum area and also identified rare alluvial ruby and sapphire grains characterised by unusually high silicon, calcium and gallium, presence of noticeable boron, tin and niobium and very low iron, titanium and magnesium contents. Oxygen isotope values ($\delta^{18}O$) for the ruby and high Si-Ca-Ga corundum (20‰–25‰) and for sapphire (10‰–20‰) indicate typical crustal values, with values >20‰ being typical of carbonate genesis. The high Si-Ca-Ga ruby has high chromium (up to 3.2 wt % Cr) and gallium (up to 0. 08 wt % Ga) compared to most Mogok ruby (<2 wt % Cr; <0.02 wt % Ga). In trace element ratio plots the Si-Ca-Ga-rich corundum falls into separate fields from the typical Mogok metamorphic fields. The high Ga/Mg ratios (46–521) lie well within the magmatic range (>6), and with other features suggest a potential skarn-like, carbonate-related genesis with a high degree of magmatic fluid input The overall trace element results widen the range of different signatures identified within Mogok gem corundum suites and indicate complex

genesis. The expanded geochemical platform, related to a variety of metamorphic, metasomatic and magmatic sources, now provides a wider base for geographic typing of Mogok gem corundum suites. It allows more detailed comparisons with suites from other deposits and will assist identification of Mogok gem corundum sources used in jewelry.

Keywords: Mogok; ruby; sapphire; trace elements; LA-ICP-MS analysis; oxygen isotopes; genetic diversity; geographic typing

1. Introduction

1.1. Mogok Gem Corundum Sources

The Mogok area, Myanmar, forms a renowned gem tract notable for its ruby and sapphire, which are recovered from both host rocks and transported deposits [1,2]. The gem mining areas recently became more accessible after 15 years of government restrictions on visits by outside personnel, which has stimulated and increased research activities on gem deposits [3,4]. Recent studies include detailed trace element based surveys of ruby and sapphire deposits [5,6]. These underpin the present follow up study, which concentrates on the trace element and O isotope characteristics of additional samples.

1.2. Trace Element Studies Background

Trace element analyses of corundum crystals provide investigative pathways into their source characteristics and crystallization conditions and are particularly useful indicators for detached gem corundum in secondary deposits [7,8]. Eluvial and alluvial transported corundum can accumulate in placers either from surrounding regional metamorphic terrains and their igneous intrusions or from underlying lithosphere when transported to the surface by later volcanic processes, so their origins can be complex [9,10]. Trace element studies when allied with O-isotope data form a powerful tool for discriminating more precise lithological sources [7,8,11–15]. Ultimately, enough geochemical testing may enable geographic typing of the corundum suites [16–18]. Gem corundum from Myanmar, particularly from the Mogok area [1], has recently received considerable attention in determining specific trace element signatures from particular lithological sources [5,6,19,20]. Two studies used comparative electron micro-probe analysis (EMPA) and laser ablation-inductively coupled plasma-mass spectroscopy (LA-ICP-MS) analysis, with one study concentrating on ruby [5] and the other on blue sapphire [19]. The other studies only presented LA-ICP-MS results, but covered a wide range of sapphire and ruby sites [6,20]. Comparisons of the data sets within these studies identified some systematic differences between the results from the two analytical methods [6]. That study showed that V-rich (V >90 ppm; V/Cr >1) ruby and sapphire exists in the Mogok area and that V-enrichments in the corundum may reflect local geographic sources. In general, the EMPA results typically gave Cr and V values 1.2 to 5 times higher than did comparative LA-ICP-MS results on the same samples. This needs attention in comparing trace element data sets. The Harlow and Bender 2013 ruby study [5] made a specific search within the analytical data for a distinctive skarn-like source trace element "fingerprint", but were unable to definitively verify such a fingerprint. The present study discusses additional corundum analyses on Mogok area samples,

not included in the present authors' initial 2014 study [6]. These were outlined at a gemstone symposium at the 34th International Geological Congress, Brisbane, Australia, 2012 [20]. Two samples had abnormally high Si, Ca and Ga which may indicate a potential skarn-like signature and are considered further here. Overall, the new samples represent both primary and secondary corundum sites. Some sites expand data from the initial sampling areas, while others represent new sampling locations. The additional analyses include further examples of high V-rich rubies, a feature of the initial study [6].

1.3. Geological Background

The settings of the gem corundum deposits are detailed within recent studies [1,5,6,19] and the geological evolution is only outlined here. Collisional terrains of granulitic gneisses and sedimentary marine sandstones and shales extend back to Late Precambrian in age. Later collisions involved Permian to Triassic (250–200 Ma) sedimentary carbonate sequences (limestones, dolomites). Metamorphism during closures of Tethyan oceans, continued into Late Cretaceous time (90 Ma). Major collision of India with Eurasia impacted a Neo-Tethyan back arc at ~60 Ma and continent-continent contact at ~40 Ma [21]. Significant tectonism within the Mogok area from 25 to 20 Ma (lithospheric rotation, major shear faulting and regional metamorphism) also led to younger granitic/syenitic intrusions (32–15 Ma) and skarn formation (as late as 19–16 Ma). Compressive Late Cenozoic uplift facilitated erosion of corundum sources and placer deposits [22]. Sites studied here are summarized in Table 1.

Table 1. Mine sites, locations and sample character, Mogok area gem corundum.

Site	Longitude	Latitude	Sample #.	Color	$\delta^{18}O$	Origin
Htin-shu-taung	96°28'40"	23°00'23.5"	H-s-t 1	Purple red	21.0	Placer
			2	Purple red		
Ohn-bin-ywe-htwet	96°32'10"	22°54'30"	O-b-y-h 1	White	22.9	Placer
			2	White		
Kyauk-saung	96°27'26"	22°55'50"	K-sa 1	Purple red	22.7	Primary
			2	Purple red		
			3	Purple red		
Htayan-sho	96°30'32"	22°57'51"	H-s 1	Blue/yellow	18.1	Primary
			2	Blue/yellow		
Chaung-gyi	96°30'32"	22°57'51"	C-g 1	Pink red	NA	Placer
			2	Mauve		
Kolan	96°26'33"	22°55'55"	K 1	Purple red	22.1	Primary
Le-shuza-kone	96°39'50"	22°58'30"	L-s-k 1	Blue	10.5	Primary
			2	Blue		
Kyauk-sin	96°25'54.9"	22°57'27.7"	K-si 1	Pink red	21.8	Placer
			2	Pink		
Yadanar-kaday-kadar	96°23'01"	22°54'30"	Y-k-k (a) 1	Red/Purple	24.2	Placer
			2	Red		
			Y-k-k (b) 1	Blue/yellow	19.9	Placer
			2	Blue/yellow		

Table 1. *Cont.*

Site	Longitude	Latitude	Sample #.	Color	$\delta^{18}O$	Origin
Manar	96°31'18"	22°58'16"	M 1	Blue	16.0	Placer
			2	Mauve		
Kyauk-poke (28)	96°26'57"	22°56'19"	K-p 1	Red	22.4	Primary
			2	Red		
Le-U (29)	96°31'28"	22°56'33"	L-u 1	Red	20.4	Placer
			2	Red		
			3	Red		

2. Sample Sites, Materials and Analytical Methods

2.1. Primary Sample Sites

Five primary corundum sites sampled in this study include three ruby sites (purple red to red; Kyauk-saung, Kolan, Kyauk-poke) and two sapphire sites (blue/yellow, blue; Htayan-sho, Le-shuza-kone). These samples came from several mining regions in the Mogok tract, except at Shwe-daing mine and Dattaw mine (temporarily closed). Dattaw ruby, however, was analyzed by Harlow and Bender [5]. Samples collected by Kyaw Thu came from seven areas where hosts show different textures and colors of marble bands and associated indicator minerals. The ruby-hosts form narrow, parallel, lenticular, *en echelon* bands in the southern flanks of hills from Dattaw to Pingu-taung.

(1) The ruby bearing marble bands at the Dattaw mines lie near the summit of the hill. The bands are very coarse grained and usually associated with fracture zones. Within the Dattaw taung area, these bands alternate with phlogopite marble and titanite (sphene)-diopside marble bands and are white, blue (medium to coarse grained) and green/yellow (medium grained) and generally ~1.2 m wide by 0.3–0.5 m across. The indicator minerals in these quarry mines include light blue scapolite, apatite, pyrite and phlogopitic mica. Fracture-filled deposits and cave deposits (secondary deposits) also occur in this area.

(2) In the Shwe-daing—Lin Yaung Chi group of mines, at Shwe-daing the upper portion of the ruby-bearing marble is blue marble and its lower portion is yellowish marble. Associated minerals are apatite and fuchsitic mica (Cr-rich mica). The ruby host is ~0.5 m thick. The lithology resembles that in the Dattaw area. At Lin Yaung Chi mine, along the tunnel (trending to the south) calc-silicate rocks are followed by yellowish marble and then medium grained ruby-bearing marble bands distributed along N 15° E and N 345° W directions. Primary ruby occurs in the marble and contact zone between yellowish marble and intrusive rocks, along with scapolite, diopside and phlogopitic mica.

(3) At Kadoke-tat—Kyauk-saung mines, the ruby-bearing marble bands trend N 10° W. Their texture is medium to coarse grained and their colors are light blue and yellowish white. The bands are lenticular in shape and are mostly associated with titanite (sphene), pyrite, apatite and scapolite.

(4) At Bawpadan—Kyauk-poke mines, the ruby-bearing marble bands usually lie between fine grained white marble and medium grained bluish and yellowish marble. The ruby-bearing bands are white to bluish white and ~1.4 m to 2.4 m wide. They are medium to coarse grained and other

minerals include pyrite, diopside, apatite and titanite (sphene). At Kyauk-poke, ruby-bearing bands are coarse grained, bluish and reddish brown and include titanite (sphene), scapolite, pyrite and apatite.

(5) At the Kolan—Pyaung-pyin—Kyauk-sar-taung mines, primary ruby occurs in brecciated zones and ruby-bearing marble bands. The breccias lie within fractures between two yellowish white marble bands and between yellowish white marble and diopside marble bands. The ruby-bearing marble is medium to coarse grained, bluish white and follows structurally controlled directions. The band is 15 cm to 0.9 m. Thick and is associated with scapolite, titanite (sphene), pyrite and fuchsite mica.

(6) At Pingu-taung mines, ruby-bearing marble bands, 0.6 to 1.5 m wide, lie between two fine grained white marble bands, as medium to coarse grained, yellowish white and bluish hosts. This area is famous for star ruby. Ruby also occurs at marble and syenite contacts in pockets or contact zones.

(7) At Baw-lone-lay—Baw-lone-gyi mines, the ruby-bearing marble bands are situated between very coarse grained white marble and fine grained yellowish white marble bands. The ruby-bearing bands are medium grained, white to yellowish white and between 0.4 to 0.9 m thick. At Baw-lone-gyi, the ruby is mostly are pinkish in color. Associated minerals are fuchsitic mica, diopside and scapolite.

2.2. Materials

The samples were mostly alluvial grains (~6%) and the others represent primary sources. They include red and purple-red ruby and blue, zoned blue-yellow and white sapphire. Grains range between 0.3–1.5 cm and vary in depths and hues of color. One ruby (Y-k-k) contains a dark purple blue core. Such sapphire-ruby composites also appear at Htin-shu-tuang [6]. Alluvial pale mauve, almost white sapphire (Ohn-bin-ywe-htwet) and ruby (Le-U) contain elongate inclusions of white minerals.

Grains were mounted in epoxy discs, mostly two but up to three per disc, and were polished for analysis (Figure 1). Care was taken in final polishing to avoid contamination from tin oxide paste.

2.3. Analytical Methods

The trace element analyses were performed using techniques developed at CODES, University of Tasmania [23]. Instrumentation include a Excimer 193nm Ar-F gas laser coupled with an Agilent 7500 cs quadrupole inductively coupled plasma mass spectrometer (ICP-MS). Ablation was performed in a He atmosphere in a Resonetics S155 ablation cell using NIST610 as the primary standard and BCR2G as the secondary standard. The laser was pulsed at 10 Hz on a 100 micron spot size with a fluence of 2 J cm^{-2}. Each analysis consisted of 30 s of background gas, followed by 30 s of ablation time counting for 10 ms on each mass. Standard data reduction procedures were used for the spot data using aluminium (52,395 ppm) as the internal standard element [24]. Spot analyses were made at core and rim positions on each of the analysed grains. Detection limits for the reported analysed elemental array were: Be (0.3), B (6.46), Mg (0.21), Al (0.58), Si (79.9), Ca (79.9), Sc (0.12), Ti (0.85), V (0.05), Cr (1.16), Fe (8.14), Ni (0.17), Cu (0.04), Zn (0.03), Ga (0.05), Sn (0.18), Pb (0.02). Other elements in the analytical array gave consistent below detection limit (bdl) values. Typical precision within the reported ppm values ranges from 5% to 20% at the 2 sigma level.

Figure 1. Color ranges of mounted samples. The scale bars represent 1 mm.

Some analyses showed rather higher elemental values than would normally be expected, so the analytical run was checked for confirmation. The Al, V, Si, Ca and B values appear accurate and analytical counts were steady throughout the analyses. The B values though low were clearly resolvable above the background. The instrument used had never ablated boron silicate glass, to keep the B background low. In general, the corundum chromophore element values mostly lie within the ranges found in recent Mogok trace element studies [5,6,19].

The O-isotope analyses of sampled corundum grains were performed by the CO_2 laser-fluorination method [25], at the Institute of Earth Sciences, Academia Sinica, Taipei, Taiwan. A Finnigan MAT 252 mass spectrometer (Thermo Fisher, Waltham, MA, USA) was employed to analyze the CO_2 gas. The results are reported as per mil ^{18}O values relative to Standard Mean Ocean Water (SMOW).

The analyzed sample weight ranges from 1.8 to 2.9 mg and the analytical precision is slightly better than F0.1x based on 17 analyses of the UWG-2 garnet standard [24], which was employed to normalize the daily data and has a suggested $\delta^{18}O$ value of +5.8‰ [25]. Detailed oxygen isotope data are listed in Table 1.

3. Results

3.1. V-Enrichment

The corundum includes low-V (<35 ppm), intermediate-V (35–90 ppm) and high-V (>90ppm) types (Figure 2), which pass into extreme V values (>1000 ppm), as was found in the initial study which characterised the Mogok region as a V-enriched corundum province [6].

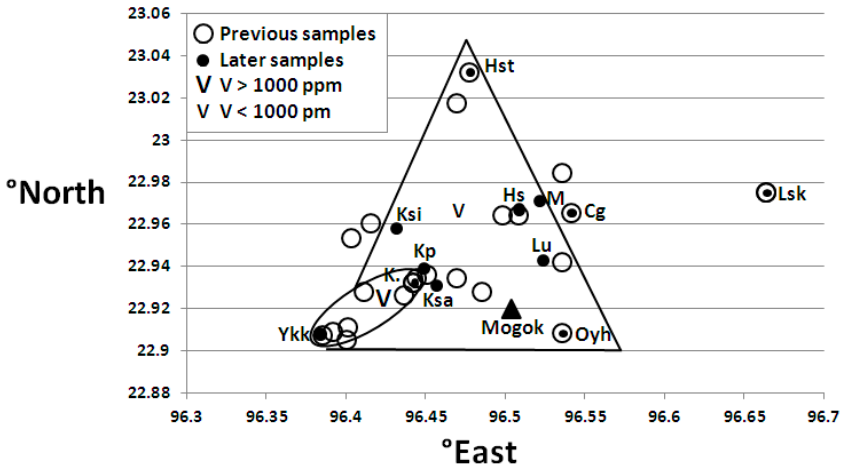

Figure 2. Locations of corundum samples analysed from the Mogok region. Samples Enclosed within the triangular zone (v) have V < 1000 ppm and in the oval area (V) have V > 1000 ppm. Localities analysed in this study (solid dots) have abbreviated symbols adapted from Table 1. Other localities (open circles) relate to the earlier study [6].

Maximum V-enrichment (1000–1400 ppm) appears within three zoned ruby samples in this study (K-sa, Y-k-k, K-p). Although these values only mark individual compositional zones within each ruby, the samples all lie within or are marginal to a designated geographic zone of highest V values in rubies within the Mogok gem province (Figure 3). Most rubies in this study show V/Cr ratios below 1 (Appendix Table A1). Some (H-s-t; K-s; Y-k-k a) shows ratios >1 (up to 7.7), but still significantly less than the highest V/Cr ratios (up to 75) found in a few enriched rubies from this zone [6]. One composite ruby-k-k), however, shows marked V (1084 ppm) and Ti (484 ppm)-enrichment relative to Cr (8 ppm) in its purple blue core zone giving V/Cr ~137 and Ti/Cr ~62 (Table A1). The core has less Fe, Ga and higher Ti than in the ruby overgrowth. Slightly elevated B, Nb, Ta and Sn (up to 3 ppm) hint at a metasomatic connection. The sapphire in this composite has more extreme V and Ti values than the sapphire enclosed in a Htin-shu-tuang composite ruby [6].

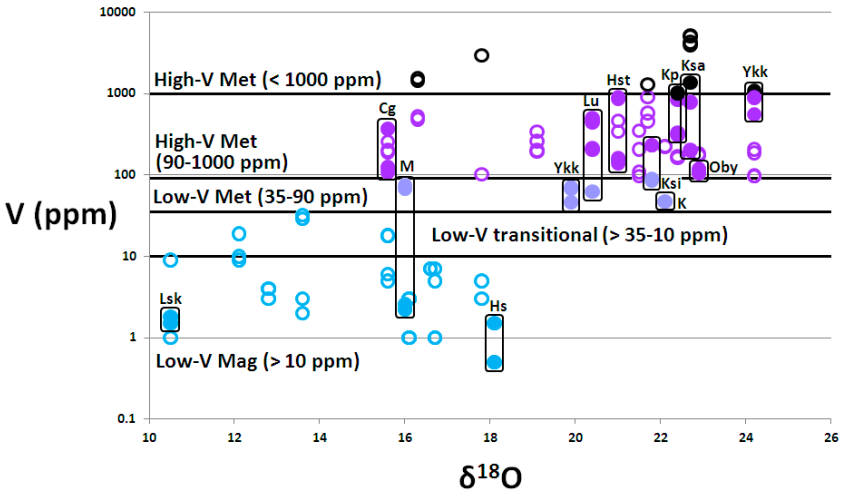

Figure 3. Vanadium (ppm)—δ^{18}Oxygen (‰) plots, Mogok corundum. Filled circles are new results (locality symbols from Table 1); open circles represent earlier results [6]. Boxes enclose results on samples from the same site. Met = metamorphic, Mag = magmatic.

Vanadium-enrichment also features in half the analysed sapphire grains (45–300 ppm) and mostly give V/Cr ratios between 2 and 96 (Appendix Table A1). This further supports the suggestion that the Mogok region represents a geographic V-enriched gem corundum province [6,20].

3.2. Unusual Trace Element Enrichments

Two of the analysed localities (pale sapphire, O-b-y-h; ruby, L-u) exhibit unusual trace element signatures. Both show exceptionally high Si (2880–4280 ppm) and Ca (1800–4600 ppm) contents. This marks a consistent feature in all ten analyses from the two samples, so needs an explanation, In general, Si-values up to about 500 ppm in Mogok rubies were considered possible incorporations within the solubility limits for the corundum structure, with higher values signifying the presence of fine-scale inclusions, or even the infusion of silica in a skarn-forming process [5]. High Ca contents are harder to accommodate in the corundum structure and the values analysed here (1797–4605 ppm) significantly exceed those normally reported from other Mogok corundum [5]. The most likely explanation for the high Si and Ca is the observed presence of white mineral inclusions, up to 6 mm long in the sapphire and 1.5 mm long in the ruby. Other features in these unusual Si-Ca-enriched sapphires and rubies are noticeable elevations (ppm) in Ga (292–802), B (11–82), Sn (2–33) and Ni (up to 16). The significance of all these enriched elemental values will be considered in discussion.

3.3. Diversity of Corundum Chemistry

The analysed corundum grains ($n = 26$) suggest a range of different chemical types can be distinguished (Table 2 and Appendix Table A1). These include: low V-ruby (V > 90 ppm; K, Y-k-k), high V- ruby (V > 90 ppm; H-s-t, Ksa,Ksi, Y-k-k a, Kp), Si-Ca-Ga-V-rich ruby (L-u), transitional Fe-rich ruby (Fe 1100–2260 ppm; H-s-t, Y-k-k b), transitional V-Cr-rich sapphire (V 105–110, Cr 125–235 ppm; C-g), transitional Ti-Mg-rich sapphire (Ti 600–660, Mg 260–280 ppm; Y-k-k b), Fe-rich sapphire (Fe 1415–8530 ppm; H-s, L-s-k, M), Si-Ca-Ga-rich sapphire (O-b-y-h).

Table 2. Multi-element LA-ICP-MS analyses, Mogok corundum. Trace element values (ppm) for the samples plotted in geochemical diagrams (Figures 2–6).

Analysis/Site	No. (r/c)	Be9	B11	Mg24	Si29	Ca43	Ti49	V51	Cr53	Fe57	Ni60	Ga69	Sn118
	1.r	<0.21	1.8	19	484	356	43	162	935	1,214	<0.19	136	0.4
H-s-t	1.c	<0.16	<1.6	21	530	362	32	138	1,009	1,097	<0.11	125	0.4
High V-ruby	2.r	<0.24	2.6	121	575	347	190	892	821	60	<0.11	52	0.3
	2.c	<0.22	3.3	156	578	370	267	863	323	71	<0.09	59	0.3
	1.r	<7.78	64.9	4	4,199	3,846	5.8	114	<0.98	0.6	9.3	292	23
O-b-y-h	1.c	<9.84	71.4	4	3,965	3,949	5.3	109	<8.9	0.6	9.4	802	20
High V-sapphire S	2.r	<13.09	<45.6	3	4,892	3,613	4.8	111	<8.05	1.1	7.2	278	30
	2.c	<13.78	81.9	4	2,879	4,605	5.5	111	<10.72	0.6	11.3	305	33
	1.r	<0.16	2.4	44	475	327	67	785	701	81	<0.09	31	0.5
K-sa	1.c	<0.21	2.8	48	251	432	72	1,373	1,603	73	<0.08	54	0.9
High V-ruby	2.c	<0.21	<2	66	293	333	99	197	4,078	81	<0.17	28	0.5
	3.c	<0.21	2.3	15	439	320	27	202	4,778	83	<0.09	29	0.4

Table 2. *Cont.*

Analysis/Site	No. (r/c)	Be9	B11	Mg24	Si29	Ca43	Ti49	V51	Cr53	Fe57	Ni60	Ga69	Sn118
H-s High Fe sapphire	1.c	0.2	1.6	55	494	421	73	0.5	4.0	8,529	<0.15	158	0.9
	1.r	<0.18	2.0	56	458	290	80	0.5	3.2	8,243	<0.1	156	0.8
	2.r	<0.16	2.5	17	435	443	28	1.5	<0.66	6,357	<0.11	127	0.3
	2.c	<0.19	2.2	17	270	319	29	1.5	<0.69	6,463	<0.08	130	0.3
C-g High V-ruby	1.r	<0.18	1.4	24	505	304	38	366	784	50	<0.07	19	0.4
	1.c	<0.16	<1.4	20	366	370	29	367	619	52	<0.1	21	0.3
	2.r	<0.19	2.4	70	416	245	149	107	107	159	<0.11	162	0.5
	2.c	<0.21	1.5	79	420	268	123	123	235	165	<0.14	176	0.4
K Ruby	1.r	<0.21	8.7	126	604	170	262	47	663	477	<0.16	84	0.2
	1.c	<0.27	10.7	125	569	297	257	47	682	496	<0.24	84	0.2
L-s-k sapphire	1.r	<0.21	<6.8	54	482	245	190	1.8	<0.52	5,307	<0.2	101	0.3
	1.c	<0.25	9.1	48	682	262	100	1.5	<0.57	4,831	<0.27	97	0.2
K-si High V-ruby	1.r	<0.17	<1.4	12	397	236	85	86	442	75	<0.09	123	0.5
	1.c	<0.18	<1.6	13	418	379	77	89	486	82	<0.15	133	0.6
	2.r	<0.21	2.4	30	424	249	46	230	757	19	<0.07	94	0.4
	2.c	<0.2	2.0	32	185	412	52	231	786	24	<0.12	97	0.3
Y-k-k (a) High V-ruby/sapphire	1.r	<0.22	<1.4	58	487	314	91	874	1,900	70	<0.14	57	0.4
	1.c	<0.21	2.8	34	559	319	484	1,084	7.8	57	<0.1	22	2.9
	2.r	<0.18	1.7	65	455	440	101	558	124	71	<0.09	29	0.5
	2.c	<0.21	2.6	59	504	326	95	908	118	47	<0.15	27	0.6
Y-k-k (b) High V-sapphire	1.r	<0.19	<1.4	34	418	282	57	47	338	2,202	0.3	118	0.5
	1.c	<0.16	1.7	34	255	319	56	46	345	2,258	0.3	122	0.5
	2.r	<0.21	<1.5	276	391	303	597	68	0.9	607	<0.17	39	0.7
	2.c	<0.23	2.3	261	464	411	659	70	<0.73	612	<0.1	41	1.0
M sapphire	1.r	<0.12	1.8	31	275	300	49	68	9.4	1,417	<0.14	75	0.3
	1.c	<0.22	2.0	31	381	325	53	74	8.5	1,558	0.1	80	0.6
	2.r	<0.15	2.0	70	528	259	195	2.2	<0.51	1,519	<0.07	61	0.7
	2.c	<0.17	1.8	91	559	254	299	2.6	1.0	1,724	<0.09	66	1.0
K-p High V-ruby	1.r	<0.15	1.7	78	551	306	124	312	995	55	<0.1	82	0.4
	1.c	<0.19	2.3	43	454	367	65	329	1,173	93	<0.08	83	0.6
	2.r	<0.15	2.2	44	365	345	66	842	6,068	135	<0.12	121	0.5
	2.c	<0.17	3.4	58	1,826	803	78	1016	3,319	134	<0.12	113	0.6
L-u High V-ruby S	1.r	<1.31	11.1	2	1,061	1,822	3.3	446	8,016	0.5	<0.45	371	2.4
	1.c	<1.96	15.2	1	2,473	2,338	3.5	63	2,066	0.1	<1.24	521	4.2
	2.r	<2.64	24.4	11	4,282	1,797	5.5	203	21,036	3.3	<1.22	506	7.8
	2.c	<4.66	<25.5	4	2,596	2,750	5.5	209	22,256	3.1	<1.74	596	5.5
	3.r	<4.42	34.3	3	2,550	1,822	4.2	212	31,674	0.8	<1.77	717	9.5
	3.c	<3.85	34.0	2	4,132	1,884	10.7	495	2,112	1.1	16.8	600	18.1

Some of these types were present among the initial Mogok sampling and analytical study [6], but the expanded data from this study includes some unusual corundum types, notably the Si-Ca-Ga-rich ruby and sapphire samples. The wide diversity in corundum chemistry now found in the Mogok field is further defined when the O isotope data for the new samples are added in with the relative levels of V-enrichments

in the corundum (Figure 3). The new plots (filled symbols) lie across an extended $\delta^{18}O$ range (16‰–22‰) and now provide a more continuous range of results, particularly within corundum V-enrichment levels between 35 and 90 ppm.

3.4. Corundum Chromophore Element Results

The relative chromophore element enrichments within the corundum for Fe, Cr and V are plotted in a triangular diagram (Figure 4). The rubies plot as low-Fe types, mostly within a range Fe/Fe + Cr + V < 0.1, but some plot with ratios between 0.1 and 0.2. The ruby plots spread along the V − Cr axis from ~V 0.95 to Cr 0.95. Titanium, as a chromophore is relatively low in the ruby, mostly <125 ppm, but extends to 270 ppm in a few cases (H-s-t, K, Kp). Higher Ti is typical in the sapphires (up to 660 ppm), particularly so in the Fe-rich dark blue sapphires (Fe up to 8530 ppm; Hs, L-s-k; Y-y-k b; M), where the blue colors are dominated by Ti − Fe^{2+} charge transfer absorption effects.

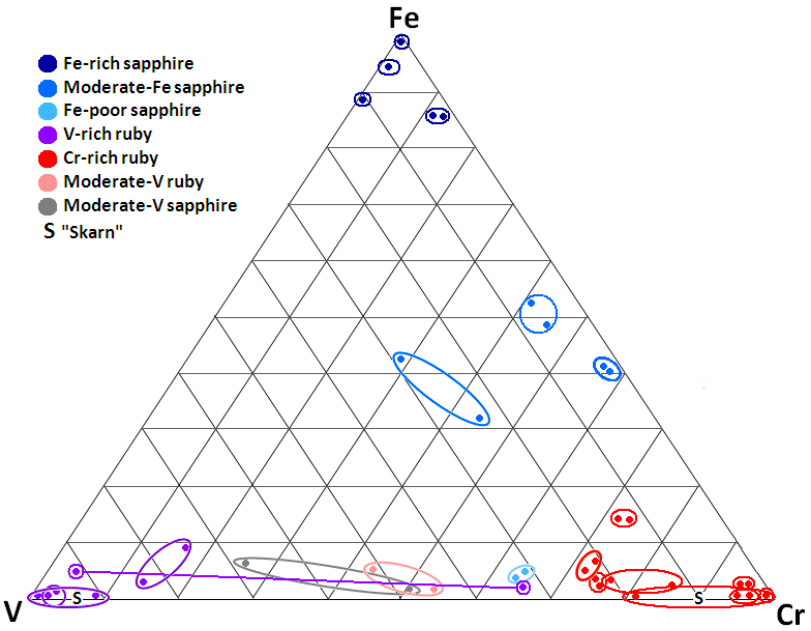

Figure 4. V–Fe–Cr Triangular plots, Mogok corundum. Oval fields encompass core and rim analyses of single crystals. The tied line connects V-rich sapphire core and ruby rim. The symbol S labels Si-Ca-Ga-rich "skarn-like" corundum.

The triangular diagram using the chromophore elements V-Fe-Cr (Figure 4) does not capture the unusual characteristics of the high Si-Ca-Ga ruby and sapphire samples, as their plots are located within the low Fe/(Fe + Cr + V) < 0.1 plots. They are designated separately by the symbol S. In contrast, within a Cr + V against Fe + Ti diagram, they largely plot away from the other corundum plots in a lower (Fe + Ti) region (Figure 6). Their (V + Cr) values (>100 ppm), however, fall in the range of the High-V metamorphic field. In Figure 4 separations between the V, Cr and Fe plots are observed. These include:

(1) low Fe-bearing corundum (Fe/Fe + V + Cr < 0.2), which includes high and low V-types and the unusual Si-Ca-Ga-rich ruby/sapphire;
(2) moderate Fe-bearing corundum (Fe 0.30–0.55, Cr 0.25–0.60, V 0. 00–0.30), which includes pink and mauve sapphire;

(3) high Fe-bearing corundum (Fe 0.85–1.00, Cr 0.00–0.12, V 0.00–0.11), which includes dark blue and blue/yellow sapphires.

The combined Fe-Cr-V results from the initial [6] and present Mogok studies, now cover a greater spread within the V–Fe–Cr triangular field, but still retains a prominent central gap between V 0.15–0.35, Fe 0.25–0.75, Cr 0.15–0.25.

4. Discussion

The overall trace element patterns in ruby and sapphire from the Mogok area, are based on recent studies using LA-ICP-MS analyses [5,6,19]. This study shows a wide diversity of geochemical signatures. The comparisons here exclude accompanying EMPA data sets, as they can produce some systematic differences among element values in the same sample [5,19]. The EMPA values often exceed the corresponding LA-ICP-MS values for Cr (1.3–5x), V (1.3–2.7x), Fe (1.1–1.5x), Ti (1.2x) and Ga (1.3x) and such differences have been attributed to operational factors within the two analytical methods [19]. Among the Mogok data sets, the ruby analyses show a wide range in V-enrichment, while the sapphire analyses show a considerable range in Fe-enrichment. Unusual trace element chemistry for Mogok sapphire was reported from Baw Mar, where it is genetically related to syenite and shows variable trace element patterns [19]. The Baw Mar sapphire ranges are not matched in the LA-ICP-MS data in this study as only ruby was analysed from that site. A near match, however, was found for alluvial blue sapphire from Shone Kan Zan [6]. This site lies about 8 km ENE of Baw Mar, but represents a different drainage area, so the similar signatures raise prospects for locating other distinctive syenitic sources for suchsapphires in the Mogok region. The expanded Mogok corundum data set now enables wider exploration of genetic associations of ruby and sapphire within this gem tract.

4.1. "Skarn" Signatures?

The highly unusual Si-Ca-Ga-rich ruby and sapphire signatures (Table 2) may mark potential "skarn" signatures (S). The pale sapphire grains (O-b-y-h) contain abundant elongate inclusions of a white mineral, which probably contribute to the trace element signature to give the elevated Si and Ca values. The signature Si/Ca ratios range from ~1 to more variable values (average Si/Ca 1.02 ± 0.35, n = 4). This suggests a calcium metasilicate mineral, most likely wollastonite, contributes to the signature. The low Mg and Fe would rule out diopside, hedenbergite and actinolite-tremolite, which are often found with wollastonite in skarn assemblages [26]. Correcting both the Si and Ca in these analyses down to more normal values up to ~500 ppm [5] would increase relative values of the other elements, but not significantly alter the high Ga/Mg ratios that normally suggest a magmatic affinity [7]. This sapphire only has faint coloration from V as the only elevated chromophore (Figures 4 and 5). The high Si-Ca, levels that accompany the calc-silicate inclusions, are accompanied by minor B, Nb, Ta and Sn contents that suggest exotic introductions.

Similar signature appears in ruby (L-u), but in contrast Cr is the main chromophore (0.21–3.2 wt %). The high Si and Ca here also suggest calc-silicate phases were involved in the ruby crystallization. Some analyses give Si/Ca ratios near 1:1, perhaps suggesting a phase such as wollastonite, but other analyses show Si/Ca ratios near 2:1, suggesting other calc-silicate phases may be present. The Cr contents are highly variable in the three analysed ruby grains and correspond with colour variation from deep red to pink.

A dark red grain has high Cr-values (2.1–2.2 wt %), a color-zoned grain with dark red rims and pale pink core passes from outer notably high Cr (3.2 wt %) to inner moderate Cr (0.2 wt %) contents and a pink grain has lower Cr (0.2–0.8 wt %) values. These ruby Cr contents are among the highest reported for Mogok rubies (LA-ICP-MS; 5, 27) and in surveys of many natural/synthetic rubies (Proton Induced X-ray Emission (PIXE), Energy Dispersive X-ray Fluorescence (EDXRF), LA-ICP-MS) where the highest Cr values were <2 wt % [27–35]. Exceptionally high Cr contents, however, are known in some unusual ruby associations [36]. In the present Mogok results Cr/V ratios range between 4 and 150 and Cr against V plots across the Group II and Group I fields into higher Cr levels [5], indicating strong chemical zoning related to these chromophores. The Ga-enrichments in this study exceed most other Mogok plots, where Ga/V is mostly <1:1 [5].

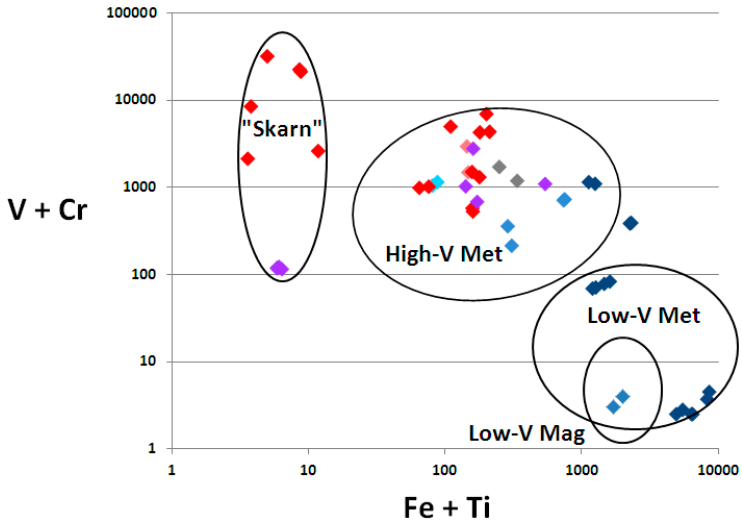

Figure 5. V + Cr − Fe + Ti plots, for Mogok corundum fields. Met metamorphic, Mag magmatic, "Skarn" Si-Ca-Ga-rich corundum.

The unusual Ga-enrichments within the high Si-Ca ruby and sapphire signatures require consideration on their source. Most Mogok and indeed SE Asian ruby genesis incorporate a metasomatic component during metamorphism of carbonate sequences which introduced the exotic trace element contents [8]. Some ruby also involves skarn metasomatic processes [1,5], although Ga enrichment is not a feature in most ruby [1,5,27–35]. Analytical aberrations caused by elemental interference effects from the Si and Ca spikes appears unlikely and compensating for the elevated values would only increase Ga values. This leaves unusual concentrations of Ga within sedimentary sources or introductions during strong igneous inputs during skarn formation as more likely alternatives. Enrichment of Ga is known to increase ~5 fold during fractionation of felsic magmas into evolved members and during greisen formation Ga becomes mobilised and disperses into fluids [37]. On balance, considering the presence of calc-silicate inclusions in the Ga-rich sapphire and ruby, a skarn-like genesis involving proximal contact with carbonate beds and a fluid–forming felsic intrusion is favoured.

4.2. Metamorphic/Magmatic Corundum Distinctions

Apart from the unusual calc-silicate metasomatic/magmatic corundum discussed above, the main Mogok ruby and sapphire suites can be assigned genetic associations based on a range of parameters.

Assignments using Cr/Ga *vs.* Fe/Ti ratios, or oxide equivalents, typically show Cr/Ga ratios <1 for magmatic origin corundum, but pass into higher Cr/Ga values for metamorphic corundum [38]. As V enrichment appears a prominent feature in Mogok corundum, a (Cr + V)/Ga parameter was used for magmatic/metamorphic discrimination [6], which assigned most magmatic sapphire to values <0.1.

Further distinctions between magmatic and metamorphic corundum, using Mg contents in blue sapphires and then extended this into ruby suites, were made using Fe or Fe/Mg against Ga/Mg discrimination plots [7,13,16]. In such plots (Figure 6), the metamorphic and magmatic fields overlap in a transitional zone between Ga/Mg ratios 3–6. This introduces some ambiguity into the genetic assignments. Within the Mogok plots, the high Fe/Mg magmatic sapphires, based on their Cr/Ga ratios, overlap into the Ga/Mg transition zone and partly into the low-V metamorphic sapphire field. Most light blue to pink sapphire and typical ruby fall within the high-V metamorphic field, with Ga/Mg ratios <3. In contrast, the Si-Ca-rich ruby and sapphire plot well into the magmatic field (Ga/Mg 46–521), suggesting some magmatic input into their crystallization.

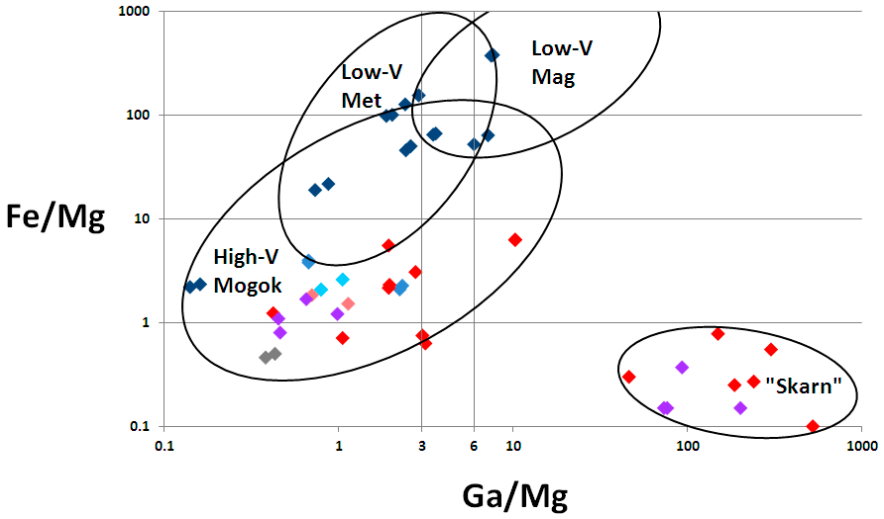

Figure 6. Fe/Mg–Ga/Mg plots, Mogok corundum.

A range of other elemental diagrams are used to differentiate isolated corundum into source associations. These include triangular plot of Mg (x100) − Fe −Ti (x10) which helped distinguish Fe-rich magmatic and Mg-rich metamorphic fields [7,13]. Some results can be ambiguous, however, so a refined triangular scheme using Fe − Cr (x10) – Ga (x100) was proposed [9]. In the present study, this scheme assigns samples L-s-k, H-s-a, M and Y-k-k to magmatic associations and most other samples into the metamorphic envelope.

4.3. Trace Element Diversity in Mogok gem Corundum Suites

Two distinctive aspects emerge from the trace element studies One is pronounced V-enrichment in many of the rubies, to >5200 ppm and V/Cr ratios >25, and in some sapphires, to >1000 ppm and V/Cr ratios up to 139. The extremes of Cr- and V-enrichment appear in a zoned composite crystals (Y-k-k a), where the V/Cr ratio (~138) in a sapphire core changes to V/Cr (0.46) in the ruby rim.

The unusual elevated Si-Ca-Ga signatures in ruby and sapphire are interpreted here as potential "skarn" signatures, but so far they are only identified in alluvial grains. "Skarn" trace element signatures in Mogok rubies were sought previously without definitive result [5]. The suspected "magmatic" skarn signatures

found in this study, however, need not preclude "skarn" origins for other ruby and sapphire that lack such a signature, as it may reflect very limited proximal effects of magmatic input. The abnormally elevated Ga, and/or Cr, V in these "skarn" signatures create problems in assigning metamorphic or magmatic affinities in some trace element classificatory diagrams. The Mogok ruby high Ga-high Cr signature is not unique, as growth banded ruby (Ga >400 ppm; Cr >4700 ppm) is recorded in alluvial grains from the New England gem-field, eastern Australia [39].

The Mogok corundum suites show transitional colors from pink and purple pink and associated brown and orange shades in sapphires into stronger purple red and red in ruby [28–30] The red in ruby results from both crystal field and co-valence effects associated with the Cr–O bond [40]. A study of ruby structures [32], showed that pink sapphire mostly involved Al–O–Cr bonds (a-$Al_2O_3 \cdot Cr^{3+}$), while ruby with more concentrated Cr contents included largely Cr–O–Cr bonds (a-$Al_2O_3 \cdot Cr^{3+} \cdot Cr^{3+}$). The proportional change in bonding shifts the color absorption effects. The ruby color is modified by other chromophore ions, such as Fe^{3+}, Ti^{4+}, Mg^{2+}, as found for Ti contents in Mong Hsu ruby [33] and significant V^{3+} in Mogok ruby [6]. The saturated red color in ruby can come from Cr contents as low as ~1000 ppm [29]. In examining the analyses of pink sapphire and ruby in the Mogok samples, either within homogeneous body color or color-zoned segments, the transition from pink sapphire to ruby takes place mostly between 1000 and 15,000 ppm Cr.

4.4. Geographic Typing of Gem Corundum on Geochemistry

Both trace element and O isotope values provide information related to the source lithology of corundum [8]. Using trace elements, metamorphic and magmatic assignments can assists in general categorization [7,39], but ambiguities and overlaps can complicate these assignments. Some studies, however, show promising geographic distinctions within restricted regions [16]. Studies of rubies from several countries, using multi-variant discrimination analysis, distinguished Myanmar rubies on their Fe and Cr contents and helped identify 63 out of 64 stones in a jewelry necklace as being sourced from Myanmar [29]. Similar trace element fingerprinting within more varied corundum suites from different gem provinces reported that both ruby and sapphire gave high degrees (up to 80%) of geographic correlation [34]. That study, however, lacked Myanmar suites. The present study suggests that high V in corundum may help support assignments of Myanmar origin.

The recent trace element studies on Myanmar, particularly Mogok, gem corundum now forms an extensive data base [5,6,19,20,30] for geographic comparisons, both local and global. Geographic typing of ruby is quite advanced [41], because of its more restricted distribution, largely confined to metamorphic sources, whereas sapphire sources are more ubiquitous [8]. This coverage may now include "skarn" signatures from Mogok.

Ruby formation may tie in with collision tectonic events [42]. Potential for skarn ruby formation, with magmatic signatures, however, may extend beyond post-deformation events. In some cases late magmatic, leucocratic and syenitic bodies may continue to intrude folded carbonate sequences. The youngest dated magmatic event within Myanmar is the Quaternary Mt Popa volcano [43], but the age of the youngest skarn corundum formation remains uncertain.

5. Conclusions

The present survey of Mogok gem corundum geochemistry provides a more comprehensive trace element and O isotope platform for geographic typing of its variations. The revealed diversity, however, undoubtedly remains incomplete. Further investigations of samples are required, particularly in relation to potential "skarn" source signatures.

Acknowledgments

Script preparation was aided by Francesca Kelly, Sydney. The script was read by Ian Graham, School of Biological, Earth and Environmental Sciences, University of New South Wales. Facilities were provided by The Australian Museum, University of Tasmania and University of Western Sydney. The Editor of *Minerals* and Guest Editors for the special issue on "*Advances in Gemmology"* are thanked for their invitation to submit a contribution for consideration. Constructive comments by G. Giuliani and two other reviewers provided improvements into the script.

Author Contributions

F. Lin Sutherland assembled data into tables and figures, interpreted the results and wrote the script. Khin Zaw designed and led the project, provided Myanmar expertise and funded analytical work. Sebastien Meffre provided technical input and ran the LA-ICP-MS analytical work. Tzen-Fui Yui provided oxygen isotope analyses of samples and technical input. Kyaw Thu provided samples for analysis and field data on Mogok localities.

Appendix

Table A1. Gem corundum V, Cr, Mg, Ga, Fe, values and ratios (ppm).

Site	No. (r/c)	V + Cr	V/Cr	V; Cr; Fe	(V + Cr)/Ga	Ga/Mg	Fe/Mg
H-s-t (4)	1.r	1,097	0.17	0.070; 0.405; 0.525	8.1	7.2	63.9
	1.c	1,147	0.14	0.062; 0.450; 0.488	9.2	6.0	52.2
	2.r	1,713	1.09	0.487; 0.463; 0.034	32.9	0.43	0.50
	2.c	1,186	2.67	0.687; 0.257; 0.057	20.1	0.38	0.46
O-b-y-h (5)	1.r	115	11.6	0.986; 0.008; 0.005	0.39	73.0	0.15
	1.c	118	12.4	0.920; 0.075; 0.005	0.15	201	0.15
	2.r	119	13.8	0.924; 0.067; 0.009	0.43	92.7	0.37
	2.c	122	10.4	0.907; 0.087; 0.005	0.40	76.3	0.15
K-sa (25)	1.r	1,486	1.12	0.501; 0.447; 0.052	47.9	0.70	1.8
	1.c	2,946	0.86	0.450; 0.526; 0.024	54.6	1.1	1.5
	2.c	4,275	0.05	0.045; 0.937; 0.018	153	0.42	1.2
	3.c	4,980	0.04	0.039; 0.944; 0.016	172	1.9	5.5
H-s (22)	1.c	4.5	0.13	0.000; 0.000; 0.999	0.03	2.9	155
	1.r	3.7	0.16	0.000; 0.000; 0.999	0.02	2.4	127
	2.r	2.5	2.27	0.000; 0.000; 0.999	0.02	7.5	374
	2.c	2.5	2.17	0.000; 0.000; 0.999	0.02	7.7	380

Table A1. *Cont.*

Site	No. (r/c)	V + Cr	V/Cr	V; Cr; Fe	(V + Cr)/Ga	Ga/Mg	Fe/Mg
C-g (9)	1.r	1,150	0.47	0.305; 0.653; 0.042	60.5	0.79	2.1
	1.c	1,046	0.54	0.334; 0.618; 0.047	49.8	1.1	2.6
	2.r	214	1.00	0.287; 0.287; 0.426	1.3	2.3	2.3
	2.c	358	0.52	0.235; 0.449; 0.315	2.0	2.2	2.1
K (10)	1.r	710	0.07	0.040; 0.559; 0.409	8.5	0.67	3.8
	1.c	729	0.07	0.038; 0.557; 0.405	8.7	0.67	4.0
L-s-k (OM)	1.r	2.8	3.46	0.000; 0.000; 1.000	0.03	1.9	98.3
	1.c	2.5	2.63	0.000; 0.000; 1.000	0.03	2.0	101
K-si (22)	1.r	528	0.19	0.143; 0.733; 0.124	4.3	10.3	6.3
	1.c	575	0.18	0.135; 0.740; 0.125	4.3	10.3	6.3
	2.r	987	0.30	0.229; 0.752; 0.019	10.5	3.1	0.63
	2.c	1,017	0.29	0.222; 0.755; 0.023	10.5	3.0	0.75
Y-k-k (a) (26)	1.r	2,774	0.46	0.307; 0.668; 0.025	48.7	0.98	1.2
	1.c	1,092	139	0.944; 0.007; 0.050	49.6	0.65	1.7
	2.r	682	4.50	0.741; 0.165; 0.094	23.5	0.45	1.1
	2.c	1,026	7.69	0.846; 0.110; 0.044	38.0	0.46	0.80
Y-k-k (b) (26)	1.r	385	0.14	0.046; 0.006; 0.948;	3.3	3.5	64.7
	1.c	391	0.13	0.045; 0.005; 0.950	3.2	3.6	66.4
	2.r	69	75.6	0.000; 0.000; 1.000	1.8	0.14	2.2
	2.c	71	95.9	0.002; 0.000; 0.998	1.7	0.16	2.3
M (27)	1.r	78	7.23	0.018; 0.131; 0.851	1.0	2.4	45.7
	1.c	83	8.71	0.017; 0.130; 0.852	1.0	2.6	50.3
	2.r	3	4.31	0.101; 0.001; 0.198	0.05	0.87	21.7
	2.c	4	2.60	0.103; 0.001; 0.896	0.06	0.73	19.0
K-p (28)	1.r	1,307	0.31	0.229; 0.731; 0.040	15.9	1.1	0.71
	1.c	1,502	0.28	0.206; 0.735; 0.058	18.1	1.9	2.2
	2.r	6,928	0.14	0.119; 0.862; 0.019	57.3	2.8	3.1
	2.c	4,335	0.31	0.227; 0.743; 0.030	38.4	2.0	2.3
L-u (29)	1.r	8,462	0.06	0.053; 0.947; 0.000	22.8	186	0.25
	1.c	2,129	0.03	0.030; 0.970; 0.000	4.1	521	0.10
	2.r	21,239	0.01	0.010; 0.990; 0.000	42.0	46.0	0.30
	2.c	22,465	0.01	0.009; 0.991; 0.000	37.7	149	0.78
	3.r	31,886	0.01	0.007; 0.993; 0.000	44.5	239	0.27
	3.c	2,607	0.23	0.190; 0.810; 0.000	4.5	300	0.55

Conflicts of Interest

The authors declare no conflict of interest.

References

1. Themelis, T. *Gems and Mines of Mogok*; A & T Publishing: Los Angeles, CA, USA, 2008; p. 356.

2. Hughes, R.W. *Ruby & Sapphire: A Collectors Guide*; Gem & Jewelry Institute of Thailand: Bangkok, Thailand, 2014; p. 384.
3. The Gem and Jewelry Institute of Thailand (Public Organization). GIT Exploring Ruby and Sapphires Deposit of the Mogok Stone Tract, Myanmar; GIT's Geologist Team under CLMV Project; Available online: http://www.git.or.th/2014/eng/testing_center_en/lab_notes_en/glab_en/2013/2013_git_exploring_ruby_sapphire.pdf (accessed on 22 December 2014).
4. Peretti, A. GRS expedition to the Mogok ruby, sapphire and spinel mines. *Jewel. News Asia* **2013**, 54–58.
5. Harlow, G.E.; Bender, W. A study of ruby (corundum) compositions from the Mogok Belt, Myanmar: Searching for chemical fingerprints. *Am. Miner*. **2013**, *98*, 1120–2013.
6. Khin, Z.; Sutherland, L.; Yui, T.F.; Meffre, S.; Thu, K. Vanadium-rich ruby and sapphire within Mogok Gemfield, Myanmar: Implications for gem color and genesis. *Miner. Depos.* **2014**, doi:10.1007/S00126-014-0545-0.
7. Peucat, J.J.; Ruffault, P.; Fritsch, E.; Bouhnik-Le, E.; Simonet, C.; Lasnier, B. Ga/Mg ratio as a new geochemical tool to differentiate magmatic from metamorphic blue sapphires. *Lithos* **2007**, *98*, 261–274.
8. Giuliani, G.; Ohnenstetter, D.; Fallick, A.E.; Groat, L.; Fagan, A.J. The geology and genesis of gem corundum deposits. In *Geology of Gem Deposits*, 2nd ed.; Mineralogical Association of Canada Short Course; Mineralogical Association of Canada: Quebec, QC, Canada, 2014; Volume 44, pp. 23–78.
9. Carter, L.E. Ruby and sapphire from Marosely, Madagascar. *J. Gemmol.* **2009**, *31*, 171–180.
10. Giuliani, G.; Ohnenstetter, D.; Fallick, A.E.; Feneyrol, J. State of the art in the formation of high-value colored stones. *Gems Gemol.* **2011**, *47*, 109–110.
11. Giuliani, G.; Fallick, A.; Rakatondrazafy, M.; Ohnenstetter, D.; Andriamamonjy, A.; Ralantarison, T.H.; Offant, Y.; Garnier, V.; Dunbigre, C.H.; Schwarz, D.; *et al.* Oxygen isotope systematics of gem corundum deposits in Madagascar. *Miner. Depos.* **2007**, *42*, 251–270.
12. Giuliani, G.; Fallick, A.E.; Ohnenstetter, D.; Pegre, G. Oxygen isotope composition of sapphire from the French Massif Central: Implications for the origin of gem corundum in basalt fields. *Miner. Depos.* **2009**, *44*, 221–231.
13. Sutherland, F.L.; Zaw, K.; Meffre, S.; Giuliani, G.; Fallick, A.E.; Graham, I.T.; Webb, G.B. Gem corundum megacrysts from East Australia basalt fields: Trace elements, O isotopes and origins. *Aust. J. Earth Sci.* **2009**, *56*, 1003–1020.
14. Izokh, A.E.; Smirnov, S.V.; Egorova , V.V.; Anh, T.T.; Kovyazin, S.V.; Phong, N.T.; Kalinina, V.V. The conditions of formation of sapphire and zircon in the areas of alkali-basaltoid volcanism in Central Vietnam. *Russ. Geol. Geophys.* **2010**, *51*, 719–735.
15. Uher, P.; Giuliani, G.; Szakáll, S.; Fallick, A.; Strunga, V.; Vaculovič, T.; Ozdin, D.; Grégaňová, M. Sapphires related to alkali basalts from Cerová Highlands, Western Carpathians (southern Slovakia): Composition and origin. *Geol. Carpath.* **2012**, *63*, 71–82.
16. Sutherland, F.L.; Abduriyim, A. Geographic typing of gem corundum: A test case from Australia. *J. Gemmol*. **2009**, *31*, 203–210.

17. Giuliani, G.; Ohnenstetter, D.; Fallick, A.E.; Feneyrol, J. Les Isotopes de l'oxygèn, un tracer des origins gééologique et/ou géographique de gemmes. *Rev. Assoc. Fr. Gemmol.* **2012**, *179*, 11–16. (In French)
18. Guliani, G.; Ohnenstetter, D.; Fallick, A.E.; Groat, L.A. Geographic origin of gems tied to their geologic history. *InColor* **2012**, *19*, 16–27.
19. Kan-Nyunt, H.P.; Karampelas, S.; Link, K.; Thu, K.; Kiefert, L.; Hardy, P. Blue sapphires from the Baw Mar Mine in Mogok. *Gems Gemol*. **2013**, *49*, 223–232.
20. Zaw, K.; Sutherland, F.L.; Meffre, S.; Yui, T.F.; Thu, K. Distinctive geochemistry among placer ruby suites, Mogok gemfield, Myanmar. In proceedings of the 34th International Geological Congress, Brisbane, Australia, 5–10 August 2012.
21. Zahirovic, S.; Müller, R.D.; Seton, M.; Flament, M. Insights on the kinematics of the Indian-Eurasia collision from global geodynamic models. *Geochem. Geophys. Geosyst. (G^3)* **2012**, *13*, 1–25.
22. Thein, M. Modes of occurrence and origin of precious gemstone deposits of Mogok Stone Tract. *J. Myanmar Geosci. Soc.* **2008**, *1*, 75–84.
23. Large, R.R.; Danyushevsky, L.; Hollit, C.; Maslennikov, V.; Meffre, S.; Gilbert, S; Bull, S.; Scott, R.; Embsbo, P.; Thomas, H.; *et al.* Gold and trace element zonation in pyrite using a laser imaging technique: Implications for the timing of gold in orogenic and Carlin-style sediment-hosted deposits. *Econ. Geol.* **2009**, *104*, 635–668.
24. Yui, T.F. Preliminary results on CO_2 laser-fluorination system for O-isotope micro-analysis of silicate/oxide grain separates. *J. Geol. Soc. China* **2000**, *43*, 237–246.
25. Valley, J.W.; Matthew, N.M.; Kohn, J.; Niendorf, C.R.; Spicuzza, N.M. WG-2, a garnet standard for oxygen isotope ratios: Strategies for high precision accuracy with laser heating. *Geochim. Cosmochim. Acta* **1995**, *59*, 5223–5231.
26. Pirajno, F. Skarn Systems. In *Hydrothermal Processes and Mineral Systems*; Springer: Berlin, Germany, 2009; pp. 535–580.
27. Mulmeister ,S.; Fritsch, E.; Shigley, J.E.; Devourd, B.; Laurs, B.M. Separating natural and synthetic rubies on the basis of trace-element chemistry. *Gems Gemol.* **1998**, *34*, 80–101.
28. Calligaro, T.; Poirot, J.P.; Querré, G. Trace element fingerprinting of jewelry rubies by external beam. *J. Nucl. Instrum. Methods Phys. Res.* **1999**, *B150*, 628–634.
29. Mittermayr, F.; Konzett, J.; Hausenberger, C.; Kaindl, R.; Schmiderer, A. Trace element distribution, solid- and fluid inclusions in untreated Mong Hsu rubies. *Geophys. Res. Abs.* **2008**, *10*, EGU-A-1076.
30. Parikh, P.; Bhardwaj, D.M.; Gupta, R.P.; Saini, N.L.; Fernandes, S.; Singhal, R.K.; Jain, D.C.; Garg, K.B. Comparative study of the electronic structure of natural and synthetic rubies using XAFS and EDAX analyses. *Bull. Mater. Sci.* **2002**, *25*, 653–656.
31. Voudouris, P.; Graham, I.; Melfos, V.; Zaw, K.; Sutherland, L.; Giuliani, G.; Fallick, A.; Ionescu, M. Gem corundum deposits of Greece: Diversity, chemistry and origins. In Proceedings of the 13th Quadrennial IAGOD Symposium, Adelaide, Australia, 6–9 April 2010; pp. 429–430.
32. Wongkokua, W.; Pongrapan, S.; Darautana, P.; Theinprasert, J.T.; Wathanakul, P. X-ray absorbtion near edge structure of chromium ions in *a*-Al_2O_3. *J. Phys. Conf. Ser.* **2009**, *185*, 1–4.
33. Pornwilard, M.M.; Hansawek, R.; Shiowatana, J.; Siripinyanond, A. Geographical origin of gem corundum using elemental fingerprinting analysis by laser ablation inductively coupled plasma mass spectrometry. *Int. J. Mass Spectr.* **2011**, *306*, 57–62.

34. Pardieu, V.; Sangsawong, S.; Muyal, J.; Chauvré, B.; Massi, L.; Sturman, N. Rubies from the Montepuez Area (Mozambique); GIA News from Research; 5 October 2013. Available online: http://www.giathai.net (accessed on 2 December 2014).
35. Sorokina, E.S.; Ozhogina, E.G.; Jacob, D.E.; Hofmeister, W. Some features of corundum ontogeny and the quality of ruby from Snezhnoye Deposit, Tajikistan (The Eastern Parmirs). *Zap. PMQ* **2012**, *6*, 95–103.
36. Giuliani, G. University of Lorraine, Vandoevre-les-Nancy, France, Personal communication, 2014.
37. Breitner, K.; Gardenová, N.; Kanický, V.; Vaculovič, T. Gallium and germanium geochemistry during magmatic fractionation and post-magmatic alteration in different types of granitoids: A case study from the Bohemian Massif (Czech Republic). *Geol. Carpath.* **2013**, *64*, 171180b.
38. Abduriyim A.B.; Kitwaki, H. Determination of the origin of blue sapphire using laser ablation inductively coupled plasma mass spectrometry (LA-ICP-MS). *J. Gemmol.* **2006**, *30*, 23–26.
39. Webb, G. Ruby suites from New South Wales. *Aust. Gemmol.* **2007**, *23*, 99–117.
40. Gaudrey, E.; Sainctavit, P.; Julliot, F.; Bondioli, F.; Ohresser, P.; Letard, I. From the green colour of eskolite to the red colour of ruby, an X-ray absorption study. *Phys. Chem. Miner.* **2006**, *32*, 710–720.
41. Keulen, N.; Kalvig, P. Fingerprinting of corundum (ruby) from Fiskenaesset, West Greenland. *GEUS Geol. Surv. Den. Greenl. Bull.* **2013**, *28*, 53–56.
42. Stern, R.J.; Tsujimori, T.; Harlow, G.E.; Groat, L. Plate tectonic gemstones. *Geology* **2013**, *71*, 723–726.
43. Maury, R.C.; Pubellier, M.; Rangin, C.; Wulput, L.; Cotten, J.; Socquet, A.; Bellon, H.; Guillaud, J.P.; Htun, H.M. Quaternary calc-alkaline and alkaline volcanism in an hyper-oblique convergence setting, central Myanmar and western Yunnan. *Bull. Soc. Géol. Fr.* **2004**, *175*, 461–472.